Research Article

Olivier Meyer*

Modelling and impact of the turbulence effect on flash and cumulative 2D active imaging system

https://doi.org/10.1515/aot-2019-0034
Received May 24, 2019; accepted July 15, 2019; previously published online August 14, 2019

Abstract: In the topic of 2D active imaging systems, two technologies exist for image acquisition. The flash mode consists of a very short and intense laser shot, associated with a short time integration of the sensor (range of hundreds of nanoseconds). The second is the cumulative mode which consists of the integration of many low level energy laser pulses over a long-time integration of the sensor (range of tens of milliseconds). Cumulative mode systems have existed for a long time in the near infrared band. But for the past few years, new sensors are available in the short wave infrared (SWIR) band. Cumulative mode in the SWIR band can provide 2D active imaging systems with very low risk considering the eye safety aspects. Moreover, with a similar design, cumulative systems can overcome the range of flash systems, thanks to their ability to average turbulence effects over the sensor integration time. So, in this paper we have proposed a scintillation noise comparison for each mode. First, we exposed the two types of available models, a numerical model, used for image generation. Second one, an analytical model, used for a quick evaluation of the design of a 2D active imaging system. Both models were compared, especially in their area of validity. Then for a specific scenario, we estimated the gain in term of range performance between a cumulative and a flash system.

Keywords: 2D active imaging; integration time; laser propagation; modelling; range performance; scintillation; turbulence.

1 Introduction

Délégation Générale de l'Armement (DGA) is mainly investigating in 2D active imaging systems for long range target identification, especially during night operations when visible electro-optic (EO) systems are not efficient (Figure 1). The task of target identification (ID) is better carried out by an active sensor compared to a thermal sensor [1] because of:

1. the lower wavelength which provides a higher optical resolution
2. the wavelength bands used (0.8× and 1.5 × μm): the active imaging allows to see the reflective contribution of materials, providing images that look a lot like a black and white visible image. The ability to see paint patterns then allows easier target identification. The contrast is higher than in IR band (mid wave infrared [MWIR] and long wave infrared);
3. they can provide better contrasted image in poor weather and obscurants compared to passive systems.

One of the disadvantages of such systems is they are non-covert. Operational use has to be defined in accordance with the threat, especially when they are equipped with a laser warning system (LWS).

Speaking now about performance, one of the main limitations for long range ID task is the atmospheric turbulence [2, 3]. As for every EO imaging systems, they can be affected by atmospheric turbulences, but active systems are affected twice:

1. On the way back (target to receiver): as other passive imaging sensors, the image is degraded by the turbulence blur (anisotropic deformation). This effect gets stronger as the field of view gets narrower (below 1°), which is the case for long range ID performances.
2. On the way forth (laser to target): because of laser coherence, the turbulence will add up a scintillation effect, resulting in a non-homogeneous laser illumination on the target plane (Figure 2, middle). This is an important effect to be modelled because it is usually the first parameter that will limit the target identification range, especially in ground to ground scenario. It results in a spatial and temporal noise on the image.

The final scintillation noise observed by the active system (or effective scintillation index) is a combination of the scintillation pattern convoluted with the turbulence and

***Corresponding author: Olivier Meyer,** DGA Maîtrise de l'Information, BP 7, 35998 Rennes Armées, France, e-mail: olivier.meyer@intradef.gouv.fr

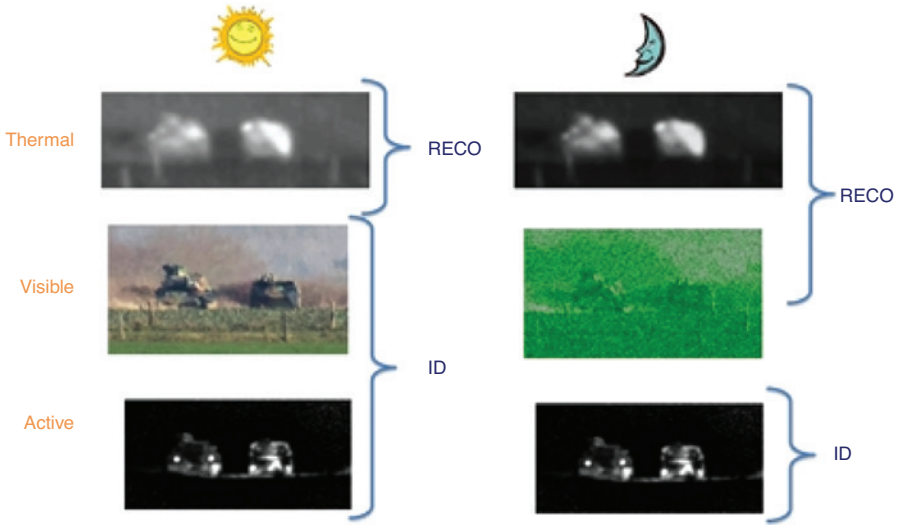

Figure 1: Benefit of active imaging sensors for target ID, especially in night operation. Every picture contains two military vehicles. Left column shows images of targets under daylight in MWIR, visible and active SWIR band. Right column shows images of targets under moonlight in MWIR, intensifying goggles and active SWIR band.

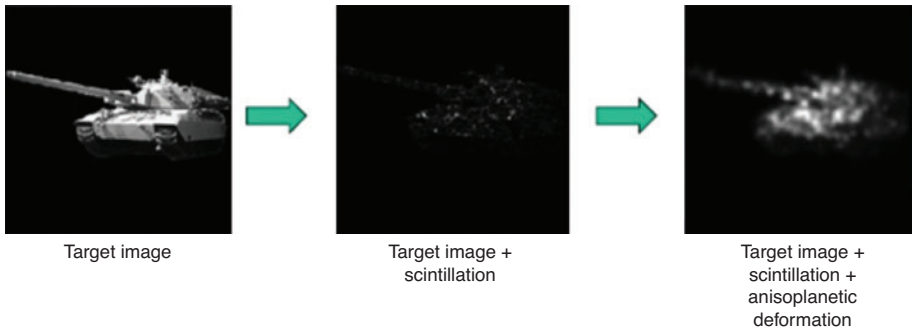

Figure 2: Turbulence effects on 2D active imaging sensor. Left: ideal image of the target. Middle: target image modulated by the laser illumination and the scintillation effect. Right: target image seen from sensor side (including anisoplanatism effect and sensor's MTF).

the camera response, e.g. optic and sensor modulation transfer function (MTF).

The gated imaging technologies can be divided into two distinct classes; single-shot, or flash imaging sensor, and multishots or cumulative imaging sensor. Single shot imagers capture the returned light from one single light pulse and forms an image, while multi-shot imagers integrate light from several returned light pulses in each image frame.

For flash system, the scintillation noise is the first parameter limiting the image quality. One of the most common image processing algorithm used to reduce it is frame averaging (Figure 3).

For cumulative system, the scintillation effect is naturally averaged, because of the longer time integration compared to flash systems (about tens of milliseconds for cumulative system versus a few hundreds of nanoseconds for flash system). So cumulative systems can provide a higher range ID performance compared to flash system, at equal system design (same energy collected per frame, same optical receiver and sensor). The temporal correlation of the scintillation is directly linked to the relative time evolution of turbulence layers between the imaging system and the target. This not only includes the transverse wind but also the transverse displacement between the target and the imaging system during the integration time in case of a dynamic scenario.

For the evaluation of active imaging range performance, DGA has several modelling tools. Some are specific to the turbulence effect, including the scintillation. They have been developed by Scalian and Onera. In this paper, we exposed:

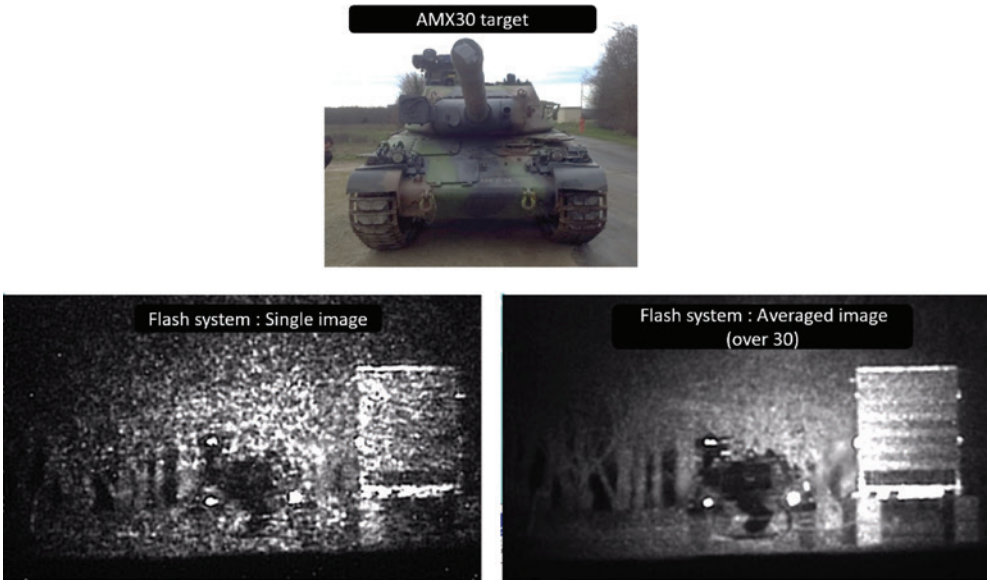

Figure 3: Flash imaging at 1.5 µm of target and chart bar panel, at a distance of 3.5 km with a field of view of 4×3 mrad. Top: close up image in the visible band. Left: target single image for the SWIR active system. Right: averaged image of the target (over 30 single images).

1. the way scintillation noise is taken into account in DGA simulation tools;
2. results coming from simulation tools to estimate the relative expected gain in signal noise ratio (SNR) between an active imaging system at 1.5 µm working in flash mode and cumulative mode based on the same characteristics.

2 Scintillation noise in modelling tools

DGA developed several tools and skills for 2D active imaging assessment:

1. by analytical modelling, for predicting target acquisition performances;
2. by image modelling, through different tools, making an end to end model.

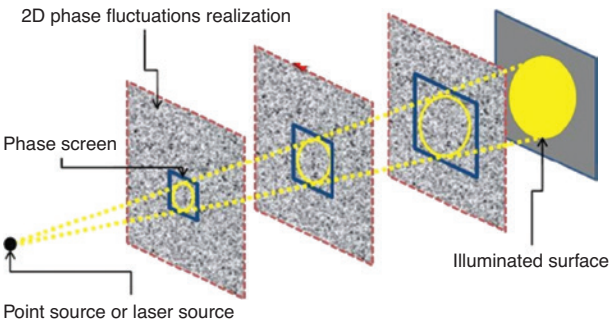

Figure 4: Principle of the screen phase propagation algorithm with the 'frozen' turbulence hypothesis.

Specific work has been conducted from 2010 up to now for the restitution of the turbulence effects (scintillation and anisoplanatic deformations) that affect flash and cumulative laser imagers with narrow field of view.

Most of the studies and prototypes are focused on flash systems at the eyesafe wavelength of 1.5 µm. But recently, new short wave infrared (SWIR) sensors started to be compatible for a use in cumulative mode. This mode has been widely used for 2D active imaging systems, using ICCD sensors, but limited to the range of near infrared band (800–900 nm). The advantage of the cumulative versus the flash mode in respect to the turbulence is the reduction of the scintillation effect. Indeed, the flash mode involves very short time integration (about 10's of ns up to 100's of ns). During this time, the temporal evolution of turbulence cells is frozen. This is not the case with the cumulative mode, it involves time integration in the order of tens of milliseconds, so the illumination pattern is averaged during the sensor time integration due to the natural turbulence layers convection movements, the transverse wind, and the relative displacement of the laser/target.

2.1 Numerical modelling tool

The numerical model, called IMOTEP (Instrument de MOdélisation de la Turbulence par Ecrans de Phase) is

based on the phase screens method, running on GPU card for fast calculation and rendering time [4–6]. IMOTEP is developed by Scalian, under DGA fundings. The phase screens propagation algorithm is based on the hypothesis of the 'frozen turbulence' i.e. very short time integration (Figure 4). One propagation of the electromagnetic field is done through the different phase screens to compute the laser illumination (or scintillation map) on the target plane.

IMOTEP scintillation maps have been validated using the theoretical expression of the scintillation index (SI) σ_I^2 defined by Andrews [7]. Scintillation index corresponds to the variance of the illumination map, when the map has a normalized value of one:

$$\sigma_I^2(z) = \frac{\langle (I(z))^2 \rangle}{\langle I(z) \rangle^2} - 1$$

IMOTEP takes into account inner and outer scales of the turbulence (l_0 and L_0) which impacts the value of the scintillation index. Simplified models neglect them (Kolmogorov spectrum of the phase variation density) which leads to under-estimating the scintillation index. Figure 5 shows the evolution of the scintillation index of a spherical wave as defined by Andrews with and without the scales of the turbulence spectrum. They are compared to IMOTEP outputs, setup with the definition of the turbulence scales ($L_0 = 2$ m, $l_0 = 1$ cm). IMOTEP outputs come from an averaged value of 100 scintillation maps for each distance step (dz = 250 m).

IMOTEP outputs fit the theoretical scintillation index with the definition of the turbulence scales. The light differences can be explained by the finite size and the resolution of the phase screens.

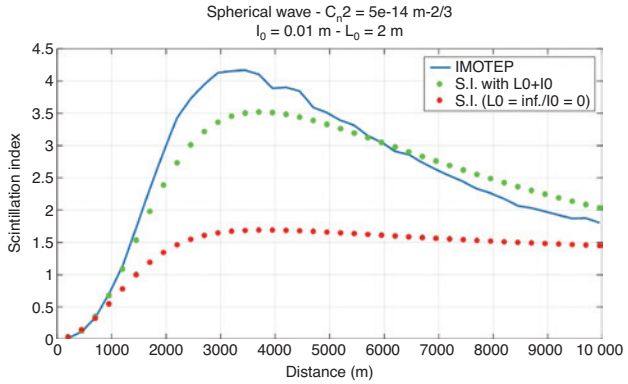

Figure 5: Comparison between theoretical models of scintillation index in spherical case (red dots curve: scintillation index under Kolmogorov phase spectrum assumption – green dots curve: scintillation index under von Karman phase spectrum assumption) and IMOTEP outputs (blue curve). Results are for a constant turbulence strength of $Cn^2 = 5 \cdot 10^{-14}$ $m^{-2/3}$ at 1.06 μm.

Analytical models are usually limited, describing the effect of the turbulence in the weak regime of the turbulence, because they are based on the Rytov approximation (scintillation index ≤ 1). The advantage of phase screens model is to reproduce scintillation effects above the weak regime.

To be a representative of the cumulative mode, the algorithm has been modified; a relative transverse displacement of the phase screens is produced during a given integration time. This displacement is calculated considering:

1. the target and/or sensor movement (case of tracking a mobile target for example);
2. the wind speed.

Then, several propagations of the electromagnetic field are carried out, and individual laser illumination maps are summed in the intensity field. Between each propagation, the screens are slightly shifted according to the relative transverse wind speed and their position in the line of sight (Figure 6).

Figure 7 illustrates the impact of different transverse wind speeds for a fixed integration time and laser pulse frequency. Four scintillation maps are displayed with the associated scintillation index (S.I.) measured on the image. They have been produced under the hypothesis given by Table 1 and are all normalized in terms of energy. Those scintillation maps have to be seen on the target plane.

In this scenario, one video frame integrates 40 laser pulses. The case '0 m/s' corresponds to a flash system. As expected, the integration process tends to smooth the scintillation pattern in the direction of the wind. Consequently, it reduces the scintillation noise.

Then, the sensor will help reducing this effect indeed, the optic resolution and sensor sampling, depending on the scenario, will reduce the scintillation. This is illustrated by adding the sensor effect defined in Table 2 on each scintillation image.

The results of Figure 7 have been updated in Figure 8 with the sensor effects. Based on the inputs of Tables 1 and 2, we plotted Figure 9, the evolution on the scintillation index measured after the detector plane for different levels of turbulence (Cn^2) and transverse wind speeds. Each point came from a set of 100 scintillation maps generated by IMOTEP, post-filtered with the representative MTF of the optic and sub-sampled in accordance to the sensor pitch.

The dotted line curve corresponds to the scintillation index for a spherical wave in the target plane. We can

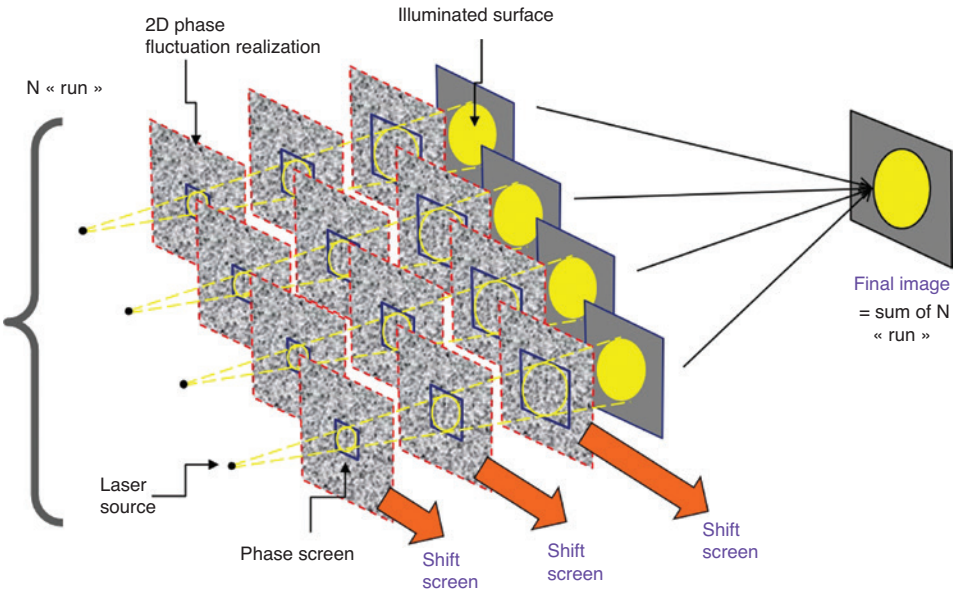

Figure 6: Principle of the new phase screens propagation algorithm outside the 'frozen turbulence' hypothesis: use of the 'frozen propagation method' N times. Between each individual propagation, the phase screens are slightly shifted according to the transverse displacement.

Table 1: Simulation inputs for time integration effect.

Parameter	Value
Distance	2000 m
Wavelength	1.55 µm
Field of view (H × V)	4 × 3 mrad
Frame time integration	40 ms (⇔25 Hz)
Laser pulse frequency	1 kHz
Pulse length	100 ns
Turbulence scales	$L_0 = 2$ m–$l_0 = 1$ cm
Cn^2 (horizontal propagation)	$5 \cdot 10^{-14}$ $m^{-2/3}$

Table 2: Simulation inputs for time integration effect with sensor effects.

Parameter	Value
Pupil diameter	10 cm
Focal length	1 m
Pixel ifov	25 µrad
Pixel sub sampling factor	8

clearly see how the wind speed helps reducing the scintillation noise.

2.2 Analytical modelling tool

Besides, the numerical model, we used an analytical model, provided by Onera, for the calculation of the scintillation index seen from the sensor side. Its advantage is the computing time. The drawback is the limitation to the weak regime of turbulence. This model is used in the analytical performance model for fast and preliminary estimation of the range performance of 2D active systems. This model is based on Onera's work [8] and adapted for DGA purposes. It involves a fully theoretical model of the power spectral density (PSD) of the scintillation index, only valid in the weak regime, with several filtering terms like:

1. The extended size of the source
2. The temporal and exposure time effect
3. The spatial filters of the receiver (optic, sampling).

This scintillation model is provided for spherical wave, and based on the von Karman DSP of the refractive index, so the inner and outer scale of the turbulence are taken into account. The spherical wavefront model is taken, because of the use of divergent laser for 2D active imaging system.

Without going into details, we can calculate the bidimensional scintillation spectrum at the detector plane, including all the spatial filtering functions starting from the isotropic spectrum of scintillation (target plane):

$$\mathrm{PSD}_{\chi}(k_x, k_y) = 2\pi 0.033 k_0^2 \times \int_0^L \mathrm{Cn}^2(z) \times \left(\left(\frac{2\pi}{\frac{LL_0}{z}} \right)^2 + k_{\perp} \right)^{-\frac{11}{6}} \times \exp\left\{ -\left(\frac{k_{\perp} L l_0}{5.91 z} \right)^2 \right\} \times \left(\frac{L}{z} \right)^{-5/3} \sin^2\left(\frac{L}{z} \frac{(L-z)k_{\perp}^2}{2k_0} \right) dz$$

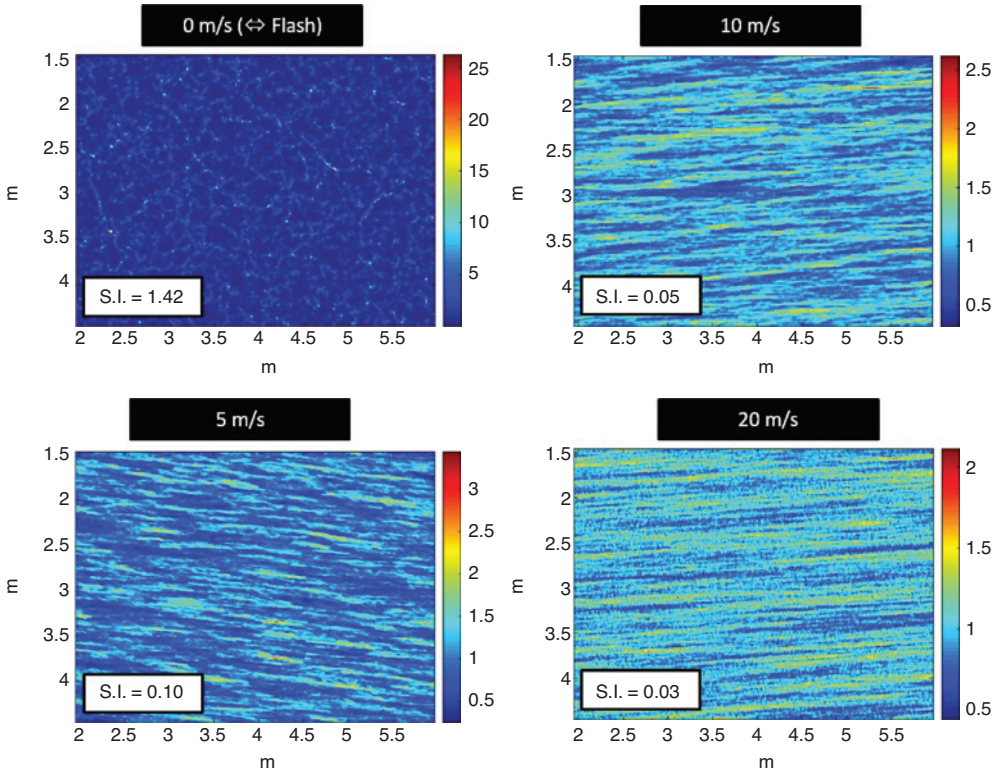

Figure 7: Scintillation map function of the relative wind speed (target plane). Each map has metric scale axis. The map size is 4×3 m.

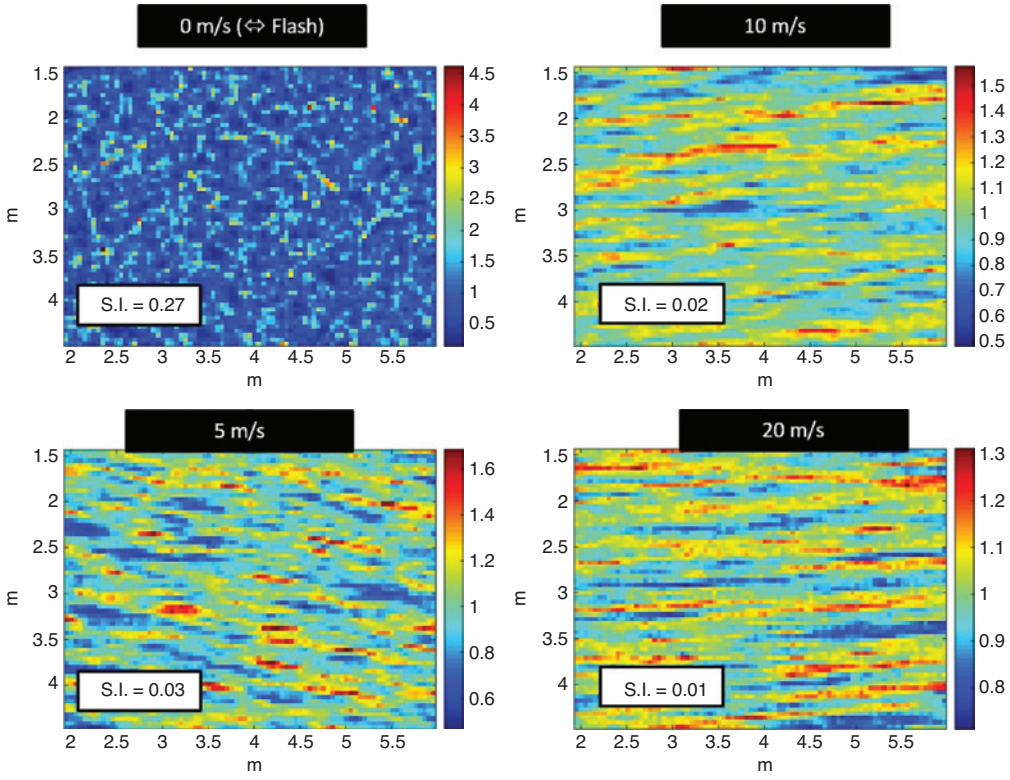

Figure 8: Scintillation map function of the relative wind speed (detector plane). Each map has metric scale axis. The map size is 4×3 m.

with the optical wavenumber: $k_0 = 2\pi/\lambda$, the source point (laser) at $z = 0$, the target plane at $z = L$, and the spatial frequencies: $k_x = \frac{2\pi}{x}$; $k_y = \frac{2\pi}{y}$ and $k_\perp^2 = k_x^2 + k_y^2$.

The scintillation index is given by the integration of PSD_χ:

$$\sigma_I^2 = 4\int_0^\infty\int PSD_\chi(k_x, k_y)dk_x dk_y.$$

The effective scintillation index is given by the integration of PSD_χ with an additional filtering term:

$$\sigma_{I_{filter}}^2 = 4\int_0^\infty\int PSD_\chi(k_x, k_y)\cdot filter(k_x, k_y, t_{exp}, v(z))\cdot dk_x dk_y.$$

The term filter $(k_x, k_y, t_{exp}, v(z))$ contains two parts:

$$filter(k_x, k_y, t_{exp}, v(z)) = filter_{exp}(k_x, k_y, t_{exp}, v(z)) \times filter_{MTF}(k_x, k_y)$$

1. Exposure time filter, for a wind across x axis:

$$filter_{exp}(k_x, k_y, t_{exp}, v(z)) = \frac{\left[sinc\left(\frac{v(z)t_{exp}}{2k_x}\right)\right]^2}{v(z)}$$

with the exposure time: t_{exp} and the transverse wind profile: $v(z)$

2. The different spatial MTFs impacting the image quality. Usually there is the turbulence, the optic, stabilization and sampling MTF:

$$filter_{MTF}(k_x, k_y) = MTF^2_{turb} \times MTF^2_{opt} \times MTF^2_{stab} \times MTF^2_{samp}.$$

Using the inputs from Tables 1 and 2, we give in Figure 10, the evolution on the scintillation index measured after the detector plane for different levels of turbulence (Cn^2) and the transverse wind speeds coming from the Onera's analytical model.

By comparing the results between the numerical and the analytical model (Figure 11), we observed that:

1. The two models give very similar results in the weak regime of turbulence.
2. Above the weak regime of turbulence, the analytical one will overestimate the effective scintillation noise.

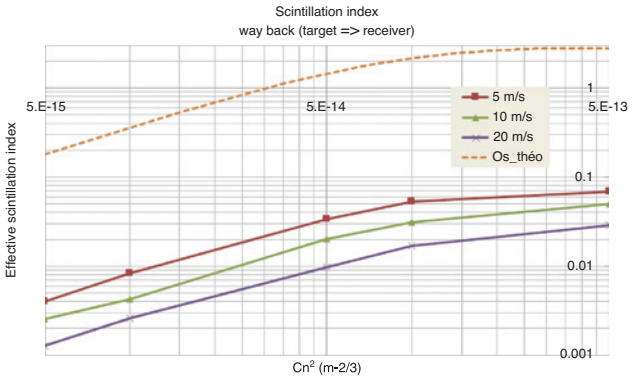

Figure 9: Scintillation index evolution depending on the turbulence strength and the transverse wind speed for the numerical model. The dotted line curve 'Os_theo' corresponds to the theoretical S.I. in the target plane for a spherical wave. The three solid line curves correspond to the effective scintillation index (detector plane) for three levels of wind speed.

If no care was taken, the analytical model could give totally wrong values for strong levels of turbulence, because the result will tend towards infinity. So, we slightly modified Onera's model in the following manner:

1. The unfiltered scintillation index in spherical wave is calculated through Andrew's law [7];
2. Then, if the filtered scintillation index calculated by the analytical model is higher than predicted by Andrew's law, we limited the output to its value.

3 Performance comparison

After the description of the models of the scintillation noise, we want to use the analytical one for a short comparison of rough range performance between a flash and cumulative 2D active imager.

For that, a simplified model of range performance is based on the SNR calculation at a specific spatial frequency. The global expression, similar to the historical Johnson model, is used:

$$SNR(f) = MTF(f)\cdot\frac{\Delta S}{\sqrt{\sigma_S^2}}$$

with:

1. f: spatial frequency in (cy/rad) or (cy/m)
2. MTF: represents all the MTF contributors. Here we took the turbulence short exposure, the optical (diffraction) and sensor sampling MTF

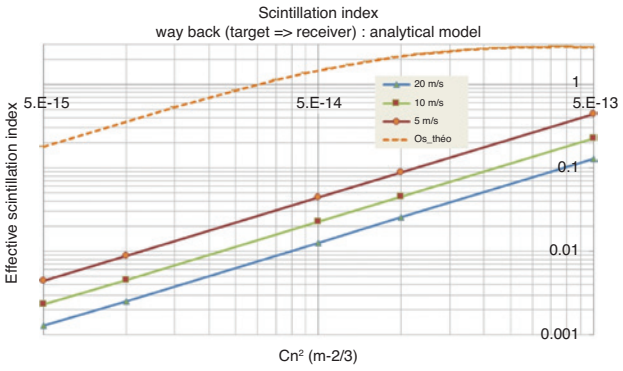

Figure 10: Scintillation index evolution depending on the turbulence strength and the transverse wind speed for the analytical model. The dotted line curve 'Os_theo' corresponds to the theoretical S.I. in the target plane for a spherical wave. The three solid line curves correspond to the effective scintillation index (detector plane).

3. ΔS: signal difference, expressed in electrons, between the target and the background
4. σ_S^2 : noise variance coming from ΔS

The scintillation index σ_I^2 corresponds to the normalized noise variance of the scintillation. Thus, the noise variance expressed in electron $\sigma_{I\,\text{electron}}^2$ is simply defined by:

$$\sigma_{I\,\text{electron}}^2 = \sigma_I^2 * ne^2$$

with *ne*, the number of electrons coming from either the target or the background. The noise is then directly related to the level of laser power deposed on the target and the background. [9] gives a more exhaustive description of the SNR. We adapt it to two main sources of noise: the scintillation and the read out noise.

$$\text{SNR}(f, z) = \text{MTF}(f, z) \times \frac{|ne_{\text{back}}(z) - ne_{\text{target}}(z)|}{\sqrt{\sigma_{ro}^2 + \sigma_{I\text{filter}}^2(z) \cdot \left(\frac{ne_{\text{back}}^2(z) + ne_{\text{target}}^2(z)}{2}\right)}}$$

with:

ne_{back}: number of electrons issued from the background (electron)

ne_{target}: number of electrons issued from the target (electron)

σ_{back}^2 : noise variance from the background (electron²)

σ_{target}^2 : noise variance from the target (electron²)

$\sigma_{I\text{filter}}^2$: Effective scintillation index

σ_{ro}^2 : read-out noise variance (electron)

The comparison is made on the same design of the flash and cumulative 2D active imaging system (Table 3). It is fair to claim that energy per frame can be equal between each technology. Today SWIR laser diode stacks can work on the level of kW with a quasi continuous wave (QCW) regime, providing similar energy as OPO SWIR laser over one video frame integration [10], and even more.

Table 3: Inputs for the working mode comparison and associated ranges.

Parameter	Value
Sensor	
Quantum efficiency	0.25
Photon-electron gain	200
Read out noise	50 electrons
Pixel size	15 µm
Time integration	40 ms for cumulative mode
	10's ns for flash mode
Optic	
Pupil diameter	10 cm
Focal length	1 m
Laser	
Energy per video frame	10 mJ
Divergence	15.4 mrad
Wavelength	1.55 µm
Target	
Background albedo	30%
Target albedo	50%
Number of bars	6
Target size	2.3×2.3 m²
Atmosphere/turbulence	
Extinction	0.1 km^{-1}
Inner/outer scale	1 cm/2 m
Cn² (horizontal propagation)	5.10^{-14} m$^{-2/3}$
Wind speed	2–5–10 m/s

Figures 12–14 present the results of the SNR versus the distance for level of transverse wind speed. For each of the three cases, the following SNR curves are displayed:

1. the unfiltered scintillation index (red dashed curve). It corresponds to the worst case in terms of range performance;
2. flash mode, i.e. very short integration time (solid red curve);
3. cumulative mode, for a 40 ms time integration (solid blue curve);
4. no scintillation effect, i.e. $\sigma_{I\text{filter}}^2(z) = 0$ (solid purple curve). It corresponds to the best case in terms of range performance.

We made the same observation as we did at the end of the Section 2.2 Analytical modelling tool; as the transverse wind speed increases, the range increases for the cumulative system due to the reduction of the effective scintillation index. Let us define a SNR threshold of 3 for the range performance. From the previous results, we plotted

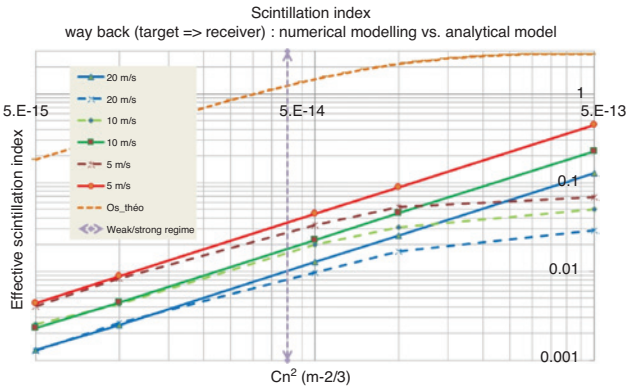

Figure 11: Model comparison of the effective scintillation index as a function of the wind speed and the turbulence level. The dotted line curves are issued from the analytical model. The solid line curves are issued from the numerical model. The orange point curve is the theoretical unfiltered scintillation index. The purple vertical line symbolises the limit of the weak regime of the turbulence.

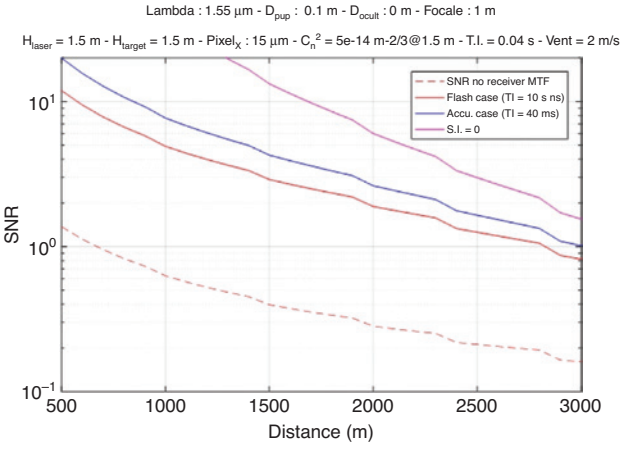

Figure 12: SNR results for transverse wind of 2 m/s.

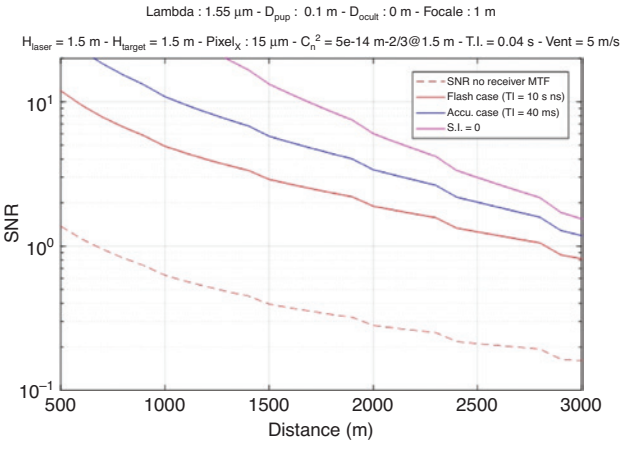

Figure 13: SNR results for transverse wind of 5 m/s.

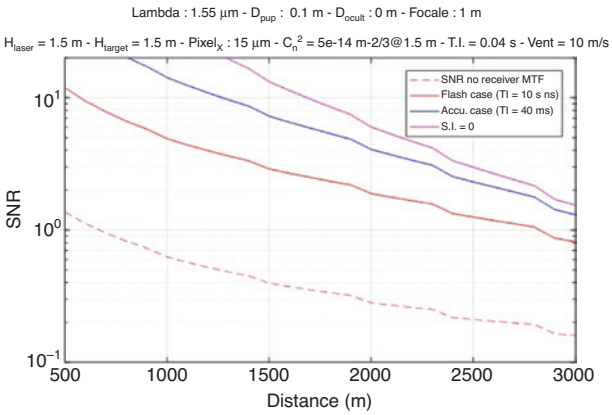

Figure 14: SNR results for transverse wind of 10 m/s.

in Figure 15 the range gain ratio of the cumulative mode compared to the flash mode as a function of the transverse wind speed (red solid curve). The maximum gain was given by the ratio between the curve without scintillation effect and the flash mode curve. This maximum gain was close to 1.7 (green dashed curve). In this scenario, for a same design (same aperture and laser energy per frame), the cumulative system has a range performance 50% superior to the range of a flash system, as the transverse wind speed is in the order of a few meters per second.

Remarks:

1. the analytical model might over-estimate the effective scintillation index. That means the red curve of the gain in Figure 15 can have a lower slope;
2. we assumed fully coherent and punctual laser source. Depending on the definition of the optical transmitter (direct emission or use of optical duct or micro-lens

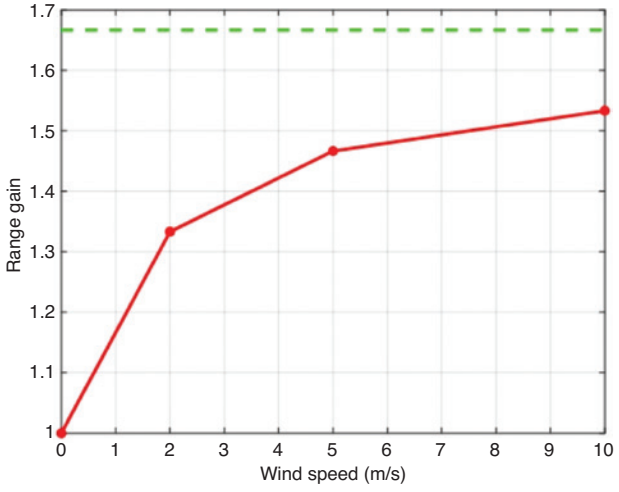

Figure 15: Gain of range performance for the cumulative mode compared to the flash mode (red curve). The maximum gain tends to 1.7 (green dashed line).

to shape the beam) and the technology of the laser source (solid state or laser diode laser), the laser coherence can be reduced and then the scintillation noise will 'naturally' be reduced as well. Such a behavior has already been mentioned by [11]. This can affect both flash and cumulative systems.

4 Conclusion

We have demonstrated the benefit of the integration time of cumulative active sensor; the scintillation noise, first noise contributor for ground to ground long range performance active sensor, is reduced. This reduction comes from the transverse time evolution of the turbulence layers. It naturally occurs due to the wind and increases if the line of sight is moving.

1. We also exposed some of the modelling tools used to estimate or render the scintillation noise. The numerical model has a higher validity area compared to the analytical model, restricted to the weak regime (Rytov regime). Cumulative systems are more robust to the scintillation effect, offering higher range performances than flash systems. Despite this gain in range, cumulative systems are also interesting for: SWAP aspect: using laser diodes or fibre lasers reduce the size of the transmitter, the consumption, and the need of cooling
2. Cost aspect: compared to solid state laser used in the flash system, laser diodes are less expensive;
3. Eye safety aspect: high frequency and low energy laser pulses will provide shorter distances of laser ocular risks compared to a single high energy laser pulse, and even more at the wavelength of 1.5 μm.

These arguments make the use of the cumulative active system technology in the SWIR band (1.5 μm) very attractive for defence and security applications. But there are two restrictions. First, cumulative systems are mainly restricted to night use, because the energy per pulse is low and their performance under daylight will be reduced. Secondly, in case of dynamic scenarios, blurring can occur if the imaging system is not stabilized for fast line-of-sight displacements. Several trials and experiments will be conducted in this way to fully estimate the benefit of the SWIR cumulative technology in France in the next few years.

Acknowledgments: I would like to thank the ISL and its active imaging team for the exchange on sensors and the laser transmitters technologies. The ONERA, DOTA Department for the development of the analytical model and my colleagues from DGA Paris for supporting and funding this work. The 'IMOTEP team' of Scalian for IMOTEP development.

References

[1] L. Hespel, Proc. 10191, 1019109 (2017).
[2] E. Jacobs and R. L. Espinola, Proc. 5987, 598703 (2005).
[3] D. Hamoir, C. Grönwall, P. Lutzmann, E. Amselem, S. Barbé, et al. 6th International Symposium on Optronics in Defense and Security (OPTRO, Paris, France, 2014) .
[4] G. Monnier and F. R. Duval, 'LASUR, an Active Infrared Synthetic Scene Generator', International Symposium on Optronics, in Defence and Security, (Paris, France, 2010).
[5] G. Monnier, F.-R. Duval and S. Amram, SPIE Remote Sensing 2012 (Edimburg 2012).
[6] G. Monnier, F.-R. Duval and S. Amram, SPIE Remote Sensing 2014.
[7] L. C. Andrews and R. L. Phillips, in 'Laser Beam Propagation through Random Media', 2nd edition (Spie Press Book, Orlando, FL, 2005).
[8] C. Robert, J. M. Conan, V. Michau, J. B. Renard, C. Robert, et al., J. Opt. Soc. Am. A 25, 379–393 (2008).
[9] E. Bernard, doctorate in the University of Toulouse, submitted 23 November 2015.
[10] Y. Lutz, E. Bacher and S. Schertzer, Opt. Laser Technol. 96, 1–6 (2017).
[11] J.-M. Poyet, O. Meyer and F. Christnacher, Opt. Lett. 39, 2592–2594 (2014).